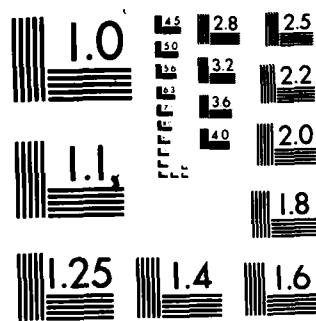MICROCOPY RESOLUTION TEST CHART

NATIONAL BUREAU OF STANDARDS-1963-A

OFFICE OF NAVAL RESEARCH

Contract N00014-81-K-0516

TECHNICAL REPORT NO. 6

Measurement of Fast Transient
and Steady State Responses
of Viscoelastic Fluids with a Sliding Cylinder
Rheometer Executing Coaxial Displacements

by

A.T. Tsai and D.S. Soong

Prepared for Publication

in the

Journal of Rheology

Department of Chemical Engineering
University of California, Berkeley,
Berkeley, CA 94720

February 9, 1984

FEB 1 7 1984

A

84 02 17 036

MEASUREMENT OF FAST TRANSIENT AND STEADY STATE RESPONSES

OF VISCOELASTIC FLUIDS WITH A SLIDING CYLINDER

RHEOMETER EXECUTING COAXIAL DISPLACEMENTS

by

A.T. Tsai and D.S. Soong

Department of Chemical Engineering

University of California

Berkeley, California 94720

Abstract

A Sliding Cylinder Rheometer (SCR) has been constructed for use with an existing Materials Test System (MTS) for the measurement of fast transient and steady-state responses of viscoelastic fluids in simple shear. Shearing is accomplished via coaxial displacement of the outer cylinder, while the inner one is held stationary. Matching pairs of circular rod and cylinder with precise dimensions, and thus well-defined annular spacings, are commercially available. The inner rod is threaded at one end for attachment to the load cell of the MTS, while flanges are welded to the outer cylinder for coupling to a cup mounted on the actuator of the MTS. Loading of the test sample is easily accomplished by raising the cup, and squeezing the fluid upwards into the annular spacing. During testing, the cup is replaced by one with large holes to eliminate pressure buildup due to compression of trapped air. This MTS-SCR combination capitalizes on the versatility and capability of the MTS programmable drive system, while the design of the SCR ensures the ideal simple shearing configuration. Experience with this new system indicates that SCR is not only less expensive to construct but also easier to use than the Parallel-Plate Rheometer (PPR) recently developed in this laboratory. The stress signals generated are reasonably free of noise. Instrumental compliance, material inertia and mechanical lag in both the input and output components of the system are minimal. Reproducible shear stress data on a polyisobutylene-in-decalin solution have been obtained for various complicated flow programs.

Introduction

In recent years there has been a constant proliferation of new rheo-metrical techniques and commercially manufactured test devices. Various geometrical configurations have been developed for studying viscoelastic fluids, such as sliding plate and cylinder, capillary, slit, couette, cone-and-plate, fiber spinning, sheet inflation and other complex flows. The strengths, limitations, and kinds of material information extractable from these existing rheometers have been extensively evaluated in a recent text by Dealy (1). Paralleling these advances in experimental capabilities is the development of network and reptation theories (2-12) to describe the rheo-logical properties of polymer melts and concentrated solutions. Particular emphasis has been placed on the behavior of such systems in transient flows. Theoretical development in turn creates further stringent demands on in-strumentation. This trend of ever-increasing sophistication of modeling and experimentation is stimulated by the constant challenge to elucidate the complex dynamics of these viscoelastic fluids in order to improve the design and control of polymer processing operations.

We report here on the development of a Sliding Cylinder Rheometer (SCR) for use with a commercial Materials Test System (MTS) for the measurement of fast transient and steady-state responses of polymeric liquids in simple shear. Shearing is accomplished via coaxial displacement of the outer cylinder, while the inner one is held stationary. Matching pairs of circular rod and cylinder with precise dimensions, and thus well-defined annular spacings, are purchased commercially. The inner rod is threaded at one end for attachment to the load cell of the MTS, while flanges are welded to the outer cylinder for coupling to a cup mounted on the actuator of the MTS. Loading of the test sample is easily accomplished by raising the actuator with

the cup mounted on it, squeezing the fluid upwards into the annular spacing. During testing, the cup is replaced by one with large holes to avoid an axial pressure gradient due to the compression of air in the cup. This MTS-SCR combination capitalizes on the versatility and capability of the MTS programmable drive system, while the design of the SCR ensures the ideal simple shearing configuration. Experience with this new system indicates that SCR is not only less expensive to construct but also easier to use than the Parallel-Plate Rheometer (PPR) recently developed in this laboratory (13). The stress signals generated are reasonably free of noise. Instrumental compliance, material inertia and mechanical lag in both the input and output components of the system are minimal, as the commercial MTS mainframe, electronics, and control loops were designed primarily for facile testing of stiff materials such as metals and ceramics. Reproducible shear stress data on a polyisobutylene-in-decalin solution have been obtained for various complicated flow programs.

Apparatus

The SCR serves as the main component for fluid confinement and testing. It is used in conjunction with the existing MTS. Figure 1 gives a block diagram of the experimental system, which illustrates the inter-relationships and functions of the various components of this setup. The rheometer is attached to the actuator below, and to the load cell above. The function generator that was originally purchased from MTS has ramp, sine, square, and saw-tooth capabilities. It is now complemented with a programmable one (Wavetek Arbitrary Waveform Generator #175), allowing an infinite number of predesignated deformation histories to be imposed on the test fluid. Either function generator can be called upon to direct the fluid displacement by means of an input signal to the actuator. The resulting vertical displacement

of the driving piston is measured with a linear variable differential trans-
former (LVDT) and the signal is fed to the servo-controller. Output from the
load cell can also be fed into this controller, so that either the stress or
the strain of the sample can be independently controlled. This versatility
plus the fast dynamics of the hydraulically-driven actuator make the MTS an
ideal instrument for transient tests. Vertical machine compliance is almost
nonexistent by virtue of the sturdy design of the load cell ($\lesssim 10^{-6}$ m under a
load of 100N). Stress and strain outputs can be either monitored on a
Tektronix 5111 dual-beam storage oscilloscope, or recorded on peripheral
recorders with fast responses such as a Linear 585 dual-beam strip chart
recorder or a Hewlett Packard 7035X X-Y recorder. These latter recorders have
been found satisfactory for faithfully tracing the output signals with
negligible time lag (13).

Detailed drawings of the rheometer are shown in Fig. 2. The basic parts
are the matching pairs of precision-made cylinder and rod, a full cup for
sample loading (left) and a perforated cup with large holes to eliminate axial
pressure buildup due to compression of trapped air (right). Two inner rods
are available to provide different gap sizes. They are both 43.18 cm long,
and are 3.818 cm and 3.970 cm in diameter, respectively. Both are threaded at
one end for attachment to the load cell. Flanges are welded to the outer
cylinder, which is 25.40 cm long and 4.092 cm in diameter, for coupling to the
cup mounted on the actuator. Loading of the sample is achieved by raising the
cup filled with the test fluid, and squeezing the sample upwards along the
annular spacing between the rod and the cylinder. Actuator upward movement is
stopped when the fluid begins to ooze out from the annular region, signaling
completion of sample loading. Once the fluid completely fills the channel,
the full cup is replaced with the perforated one for actual testing. Cup

replacement is achieved by first loosening the bolts fastening the cup and the outer cylinder. The actuator is then lowered while the outer cylinder is held fixed. Fluid trapped between the annular region separates from the reservoir in the full cup. Residual liquid clinging to the portion of the inner rod that extends outside the confines of the outer cylinder is wiped off carefully to ensure a smooth free boundary at both ends of the rheometer assembly. The ends of the annular region are thus open to the atmosphere. The fluid is held in place by its high viscosity and surface tension.

Operating Range

The two combinations of rod and cylinder in our laboratory give gap separations of 0.137 cm. and 0.061 cm. These small dimensions offer several advantages. First, data analysis can be facilitated by assuming that the shear field is uniform within the annular spacing, a point that will be justified later. Second, the fluid can be easily retained by virtue of its high viscosity and surface tension. Finally, small rates of actuator displacement translate into reasonably large shear rates, inducing large stress signals. Hence, this geometric feature allows a wide range of shear rates to be realized. Fluids with different viscosities may be tested optimally with other gap dimensions. The two available pairs of concentric cylinders allow a maximum shear γ_{max}, of about 46 and 103 strain units, respectively. This maximum shear, γ_{max}, is restricted by two major considerations. First, the limitations of the actuator design put an upper bound on its vertical travel. For our instrument, this maximum travel is about 6.3 cm from the neutral position in either direction (i.e.,a total possible displacement of about 5 in.), giving rise to the above reported γ_{max} for the two dimensions. The second, and perhaps more relevant, consideration is the condition of fluid free boundary when the sample is sheared to such large extents. The free

surface may be significantly distorted as to introduce erroneous force readings. In addition, loss of wetted surface area between the cylinders may cause the recorded force to drift downward with increasing shearing (an expected phenomenon that in principle can be corrected for in data analysis). Our experience suggests that the fluid is well retained in these small gaps of the total length of the outer cylinder). The measured load cell signal at a constant $\dot{\gamma}$ remains reasonably constant without noticeable drifts once rheological steady state is reached. Thus, in practice, γ_{max} in the neighborhood of 50 is easily achieved with the test samples used in this study. We have, in fact, pushed this upper limit to about 65 in the case of interrupted flow (to be shown later). Beyond this level, the recorded stress indeed begins to drift steadily downward, indicating attrition of wetted surface area. The maximum strain that can be achieved in the rheometer can be increased via the use of a longer cylinder pair with a smaller gap. The total shearing time at a given shear rate, $\dot{\gamma}$, is then limited to $\gamma_{max}/\dot{\gamma}$. This time restriction sometimes precludes the attainment of steady state, since fluids with long relaxation times may still be in a transient condition at the end of this time. If steady state at a given $\dot{\gamma}$ is desired, the fluid may be first sheared at a higher rate, sufficiently degrading its structure (or entanglement density) to allow subsequent rapid approach to steady state when the shear rate is reduced to the assigned $\dot{\gamma}$. Care must be exercised to ensure that the initial period of high $\dot{\gamma}$ is kept short so as not to over-destroy the fluid structure. A certain degree of experience must be accumulated through trial-and-error before this task can be accomplished efficiently. The operating $\dot{\gamma}$ range at which steady state property can be recorded is thus greatly expanded. This same strategy was found to be applicable to the PPR experiments (13).

The low $\dot{\gamma}$ limit is caused by the ability of the load cell to detect tensile (or compressive) forces generated by shearing the test fluid. The MTS load cell (manufactured by LeBow to meet standards set by MTS) used in this work has a maximum capacity of 1000 lb. The signals, however, can be amplified by using the following full-scale ranges: 0-100 lb, 0-200 lb, 0-500 lb and 0-1000 lb. Force signals can be optimally recorded by judiciously choosing the correct range. Resolution of force reading is easily at the level of 0.1 lb by using the highest sensitivity scale, (i.e., a full scale of 100 lb.). Accuracy of the recorded force is better than 0.5% (usually 0.1%) of the range selected for our study. This again translates into measurement accuracy of better than 0.5 lb. (usually in the neighborhood of 0.1 lb.). Since the total wetted surface area of the CCR is 310 cm^2, materials with viscosities higher than $10^3 Ns/m^2$ (Pa·s) at low shear rates can be easily tested with this load cell at $\dot{\gamma}$ as low as 10^{-2} sec^{-1}. Another practical limit is the possibility of fluid gradually flowing out of the gap by gravity. The problem is particularly severe when the surface tension is weak. However, for sufficiently viscous fluids, gravity flow is insignificant during the period of testing. Our experience with samples having viscosities on the order of 10^3 Ns/m^2 (Pa s) at low shear rates indicated that gravity flow was not a problem. The sample could even be left in the device for hours before resuming testing. This observation also suggests that solvent evaporation (provided the solvent is not very volatile) is not a problem either, as the rheometer is only open to atmosphere at the ends, which have an extremely small area.

The high-$\dot{\gamma}$ limit achievable by SCR is imposed by the maximum speed of the driving unit of MTS, which is approximately 13 cm/sec for our machine, corresponding to a maximum shear rate of about 208 sec^{-1} for the smaller gap

available. Machines with stiffer design and higher hydraulic pressure can improve this limit. Other considerations such as viscous heating and melt fracture may lower this upper bound. However, the use of metallic cylinders with small gap dimensions reduces the severity of temperature rise (1). In addition, the test time at high $\dot{\gamma}$ is extremely short. This also minimizes viscous heating. Melt fracture and fluid detachment from cylinder surface are realistic threats. Data must be reproduced and checked against other rheometers. For our test samples, there is no evidence suggesting the occurrence of such phenomena. We note that the sliding-cylinder geometry enjoys advantages over rotational devices, where secondary flows restrict attainment of high-$\dot{\gamma}$ simple shearing. The use of capillary rheometers greatly expands the $\dot{\gamma}$ range. However, stress transients from these systems do not provide meaningful rheological information.

Experimental

Polyisobutylene (Vistanex L-100 from Exxon Chemicals) cubes (8 cm^3) were dissolved in decalin (decahydronaphthalene) to make 20% by weight solution. Analysis of GPC of Vistanex L-100 done in our laboratory gives $M_n = 4.6 \times 10^5$ and $M_w = 1.02 \times 10^6$. Solution preparation was achieved by gentle rotation of the container (2 cycles/min) in a 70°C oil bath. Two weeks were required for complete dissolution.

The test solution at about 60°C was poured into the cup. Caution was exercised to ensure bubble-free solution transfer. The sample was loaded by squeezing the solution into the annular region. After loading, the outer cylinder was held stationary, and the cup replaced with the perforated one for testing. The desired shearing function was chosen and testing initiated. During a run, the piston displacement (measured by the LVDT) and the corresponding stress from the load cell were continuously recorded with both the

dual-channel strip chart recorder and the dual-beam storage oscilloscope. When large-amplitude oscillatory flow was under study, the XY recorder was used to obtain Lissajous figures.

All experiments were conducted in a temperature-controlled room at 24°C. A temperature chamber to surround the rheometer was available and could be used for experiments up to 250°C. One could envision jacketing the outer cylinder and circulating thermostatted liquids to achieve thermal regulation. This would only slightly complicate the current design.

Sources of Error

Ideal simple shearing is approached only if the sample is confin tween boundaries that are truly parallel during testing. Since the gap dimension is much smaller than the radius of either cylinder (the ratio being on the order of 3.0% and 6.7%), device curvature can be neglected in data analysis. For our rod-and-cylinder combinations, the assumption of a linear velocity profile instead of the more exact profile (for Newtonian behavior) would only incur approximately 1.5% and 3.4% error in $\dot{\gamma}$ at the wall. The flow field is thus a homogeneous one, provided the cylinders are exactly coaxial. This requirement was met by checking the circumferential gap uniformity of the upper opening of the annular region with nylon inserts, while loading and tightening the bolts coupling the flanges of the outer cylinder and the perforated cup. Still, there was a remote possibility for the cylinders to "yaw," i.e., tilting of the axes so they are not colinear. This orientation alignment was perfect, as the stress curves for flow in both the forward and reverse directions are entirely superimposable. (Previously, we used the same test to check alignment of the PPR (13)). This stringent test was done by first shearing the fluid in one direction and then allowing it to relax for

a long time to recover its equilibrium structural state (entanglement density). The flow was then reversed, but the same $\dot{\gamma}$ history was followed. The original stress trace, albeit in the reversed direction, was reproduced exactly.

Other potential sources of experimental error were also precluded. The sturdy construction of SCR not only made axis tilting an unlikely eventuality, but also imparted almost zero mechanical compliance. In order for controlled fast transient programs to be faithfully executed, overall compliance of the various parts of the rheometer must be kept minimal. This requirement brings out one of the outstanding features of MTS. The load transducer is the softest link of the entire load train, giving a deformation of 7.6×10^{-5} m under a full load of 1000 lb. Equivalently, a displacement on the order of 10^{-6} m is expected under a load of 100N, the force range encountered in our study. The MTS frame itself and various couplings in the rest of the load train would give only 1.8×10^{-4} m under a tremendous load of 22000 lb. This rigidity is not easily matched by other systems. In fact, conventional rotational devices using torsion bars to produce electrical signals often suffer from this deficiency. In contrast, the MTS load cell is constructed chiefly of a high-strength piezoelectric metal column; the deformation induced by the applied force is vanishingly small for our experiments. The mechanical lag in the input and output components of the MTS, which was originally designed for testing solids, has been found to be minimal as well (13). We note here that LVDT is an inductive transducer, a phase lag may be inadvertently introduced between the actual stroke and the recorded piston displacement. This is apparently not a problem for frequencies lower than 100Hz or so. High frequency testing would require more elaborate electronics to eliminate this phase shift through empirically determined correction

factors. We only report data at reasonably low frequencies, so this complication is avoided.

Still, another potential factor compromising the quality of our data is the errors introduced by the distorted free surface at the open ends, a point worth careful examination here. We have previously stated that the recorded stress can be maintained at a constant level in steady shearing up to displacements as large as 10% of the rheometer length, a somewhat surprising observation. Here, we offer partial explanation for this, following Laun and Meissner's argument (14). These authors constructed a sandwich-type creep rheometer, where the typical rheological response of the fluid is on the order of $100N/m^2$. Errors due to surface tension would amount to 1.8% of the measured signal. Typical rheological response for our system is on the order of $1000N/m^2$, and our rheometer has a substantially less fraction of free surface. The possible errors due to surface tension of the distorted boundaries at the ends must be even more insignificant than those introduced in the sandwich rheometer.

A convincing test of the accuracy of data generated by the SCR is shown in Fig. 3. Results of $\dot{\gamma}$ -dependent steady-state viscosity from this instrument agree well (to within ± 4.4%) with those obtained previously on the PPR (13). The experimental data were collected over several runs on different days, showing consistent reproducibility of the apparatus. The PPR data have been compared with dynamic tests performed on the same solution using a Weissenberg Rheogoniometer. The sample was found to obey the empirical Cox-Merz rule (13). This agreement of results among three devices strongly supports the reliability of the data from the CCR on an absolute basis, free from instrumental artifacts, misalignment, and end effects.

Results

The ability of SCR to carry out fast transient tests is attested in
Fig. 4, which shows the results of stress growth and relaxation experiments on
both PPR (13) and SCR. The role of PPR is identical to that SCR in many
respects. It is also represented by the block marked "Rheometer" in Fig. 1,
and can be used inter-changeably with SCR. However, in general the stress
trace from PPR is marred by minor fluctuations during flow, as shown here for
the stress growth period. A smooth relaxation curve is nevertheless
obtainable. In order to ensure a fixed gap distance between plates during
testing, the plates must be mechanically coupled. This was achieved in our
design of PPR by attaching the plates to Thomson ball bushings riding on
precision guide rods on both sides of the assembly. The precautions thus
taken restricted the potential plate separation due to normal forces produced
by shearing (13). However, even the very slight rolling frictional drag of
the bushings is reflected in the resulting stress trace. The fluctuations are
nevertheless small enough to permit ready determination of an average, smooth
stress growth curve. The SCR, in contrast, has no moving mechanical parts in
direct contact. The only coupling between the rod and the outer cylinder is
through the test fluid confined in the annular spacing. A smooth stress trace
is therefore always attainable with this device. (The amplifier and associated
electronics of MTS generate on the average a noise level of 25mV for a full
range of 10V). Figure 4 demonstrates unequivocally the agreement between the
two rheometers in generating transient data and the superior quality of such
results from SCR.

A number of other transient experimental data sets are presented in
Figs. 5-9. The strain programs presented here include step reduction and
increase in shear rate, interrupted flow and large-amplitude oscillatory

flow. Stress transients induced by such controlled experiments are in good agreement with results of PPR (13) and predictions of a kinetic network model developed in this laboratory (9, 15-18). The observed transient behavior and its structural and rheological implications were discussed elsewhere (9,17). Our main objective here is to illustrate the range of capabilities of the SCR. Other controlled transient experiments have been conducted with PPR (13,19), such as pre-steady-state stress relaxation, repeated flow reversal, steady shearing preceding and following oscillation, steady shearing with superimposed oscillation, and exponential increase in shear rate. These more complex transients are equally feasible with SCR.

Relative Merits of SCR and PPR

We will now summarize the relative advantages and disadvantages of SCR and PPR. Several points are noted below.

1. Loading of sample is significantly easier with SCR than PPR. Great care is required to ensure complete surface coverage, bubble-free condition, and precise plate alignment during closure of PPR. In contrast, sample loading and instrument alignment of SCR are relatively painless.

2. The plates of PPR must be held together via mechanical means to avoid gap thickness variation due to normal forces, while the rigid surface of the cylinders obviates this complication.

3. SCR generates stress signals free of noise, as it has no contacting moving parts. PPR traces are slightly inferior; the use of Thomson ball bushings travelling along precision guide rods minimizes extraneous frictional drag, but still leads to fluctuating stress signals.

4. Both SCR and PPR are susceptible to potential end effects, but edge effects are possible only with PPR. The PPR design must be such that the thickness is much smaller than both its length and width. The gap dimension of SCR must be small compared to the cylinder radii to facilitate data analysis.

5. SCR only permits shear stress measurements, whereas the use of a flush-mounted transducer on PPR in the center of the plate away from edges in principle permits normal force measurements as well. For a more well-defined rheological quantity, hole pressures could be used to estimate N_1.

6. Operating $\dot{\gamma}$ range is comparable for both rheometers. Viscosity master curves for most fluids of interest can be delineated with either device. The cost of construction is, however, much less for SCR than PPR.

Conclusion

In conclusion, a versatile rheometrical technique has been devised to determine fast transient and steady-state responses of viscoelastic liquids in simple shear. A few representative sets of data on a 20% by weight PIB-in-decaline solution have been presented. This device is currently employed to measure rheological properties of solutions of different concentrations and viscoelastic responses following step and multiple-step strains. These results will be reported in future publications. We have also begun to explore the possibility of obtaining nonlinear creep data by exploiting the stress-control mode of MTS.

Addendum

Rheometers similar to SCR have been employed to measure the viscosity of molten polymers at low $\dot{\gamma}$ (20) and to extract their dynamic mechanical properties (21). The latter design by McCarthy utilized an ingeneous sample filling (by extrusion) technique and allowed both axial and rotational oscillation to be examined. However, the use of SCR to obtain fast transient and steady-state viscosity data over a wide $\dot{\gamma}$ range has not been achieved before.

In addition to reporting on SCR, we will compare this apparatus with the falling cylinder geometry where considerably more complicated flow prevails at one end. Fluid flow in SCR is couette in nature, whereas flow in falling cylinder devices is induced by both drag and pressure. The simple flow pattern in SCR allows approximate analysis of the rheological data from this instrument easily. Rigorous analysis of data must account for cylinder curvature as $\dot{\gamma}$ is strictly a function of radial position (1). However, since our gap width is much smaller than the cylinder radii, $\dot{\gamma}$ becomes nearly uniform and the raw data can be analyzed accordingly. The assumption of a homogeneous flow field is supported by the observation that viscosity data obtained using either available gap size agree with each other.

In contrast to the simplicity of SCR, a geometrically closely related but fundamentally distinct class of rheometers, the falling cylinder devices (Fig. 10), are much more complex inherently. These systems have an inner rod pushing against the fluid contained in the outer cylinder with its lower end capped. The inner cylinder may fall as a result of a fixed weight placed on it (22-26) or may be driven by a mechanical testing device (27,28). A number of undesirable features associated with this type of rheometers make it difficult to analyze the raw data. First, fluid flow in the annular space is promoted by both cylinder displacement and pressure buildup in the liquid

reservoir. The velocity profile is thus a nonlinear function of radial position and $\dot{\gamma}$ is not uniform (Fig. 10). Determination of $\eta(\dot{\gamma})$ must presuppose a known functional form, e.g., Newtonian (22) or power-law behavior (23), whereas the actual $\dot{\gamma}$ of the fluid in the annular spacing may span both Newtonian and non-Newtonian regimes at high speeds of rod travel. Second, an end correction (25) must be introduced to allow for the fact that the liquid does not reach its fully developed velocity profile immediately upon flowing into the annular space from the bottom of the outer cylinder. Two additional potential sources of error have been identified in Fig. 10, those due to converging flow near the entrance to the annular region and squeezing flow between the bottom of the rod and the end of the outer cylinder. For highly elastic fluids at high flow rates, the force measured on the inner rod may be greatly affected by the details of the converging section and the gap separation of the squeezing flow region. It is not clear at present how all these complications can be accommodated in analyzing transient data.
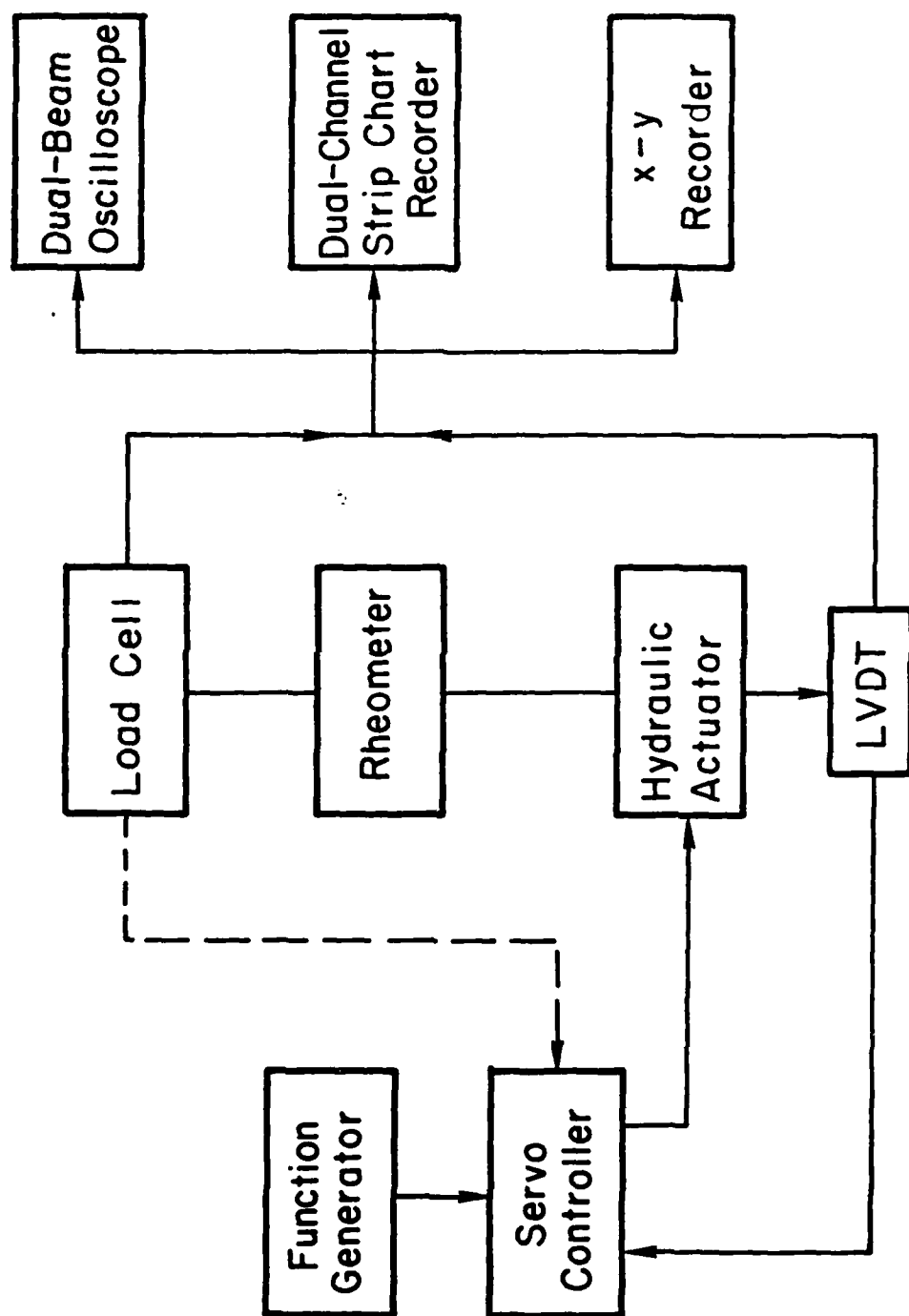
Acknowledgement

References

1. J.M. Dealy, "Rheometers for Molten Plastics," van Nostrand Reinhold, New York, 1982.

2. D. Soong, Rubber Chemistry and Technology, $\underline{54}$, 641 (1981).

3. R.B. Bird, Physica, $\underline{118A}$, 3 (1983).

4. M.H. Wagner, Rheol. Acta, $\underline{18}$, 33 (1979).

5. D. Acierno, F.P. La Mantia, G. Marrucci, and G. Titomanlio, J. Non-Newtonian Fluid Mech., $\underline{1}$, 25 (1976).

6. D. Acierno, F.P. La Mantia, G. Marrucci, G. Rizzo, and G. Titomanlio, J. Non-Newtonian Fluid Mech., $\underline{1}$, 147 (1976).

7. R.J.J. Jongschaap, J. Non-Newtonian Fluid Mech., $\underline{8}$, 223 (1981).

8. J. Mewis and M.M. Denn, J. Non-Newtonian Fluid Mech., $\underline{12}$, 69 (1983).

9. T.Y. Liu, D.S. Soong, and M.C. Williams, Polym. Eng. Sci., $\underline{21}$, 675 (1981).

10. Doi and S.F. Edwards, J. Chem. Soc. Faraday Trans., $\underline{74}$, 1789, 1802, 1818 (1978), $\underline{75}$, 38 (1979).

11. G. Marrucci, in Advances in Transport Process, $\underline{V}$, A.S. Mujumda, R.A. Mashelka, eds., John Wiley and Sons.

12. C.F. Curtis, R.B. Bird, and H.H. Saab, J. Chem. Phys., $\underline{74}$, 2016, 2026 (1981), J. Phys. Chem., $\underline{86}$, 1102 (1982), J. Chem. Phys., $\underline{77}$, 4747, 4758 (1982).

13. T.Y. Liu, D.W. Mead, D.S. Soong, and M.C. Williams, Rheol. Acta, $\underline{22}$, 81 (1983).

14. H.M. Laun and J. Meissner, Rheol., Acta, $\underline{19}$, 60 (1980).

15. D.S. Soong and M. Shen, J. Polym. Sci., Polym. Letters, $\underline{17}$, 595 (1981).

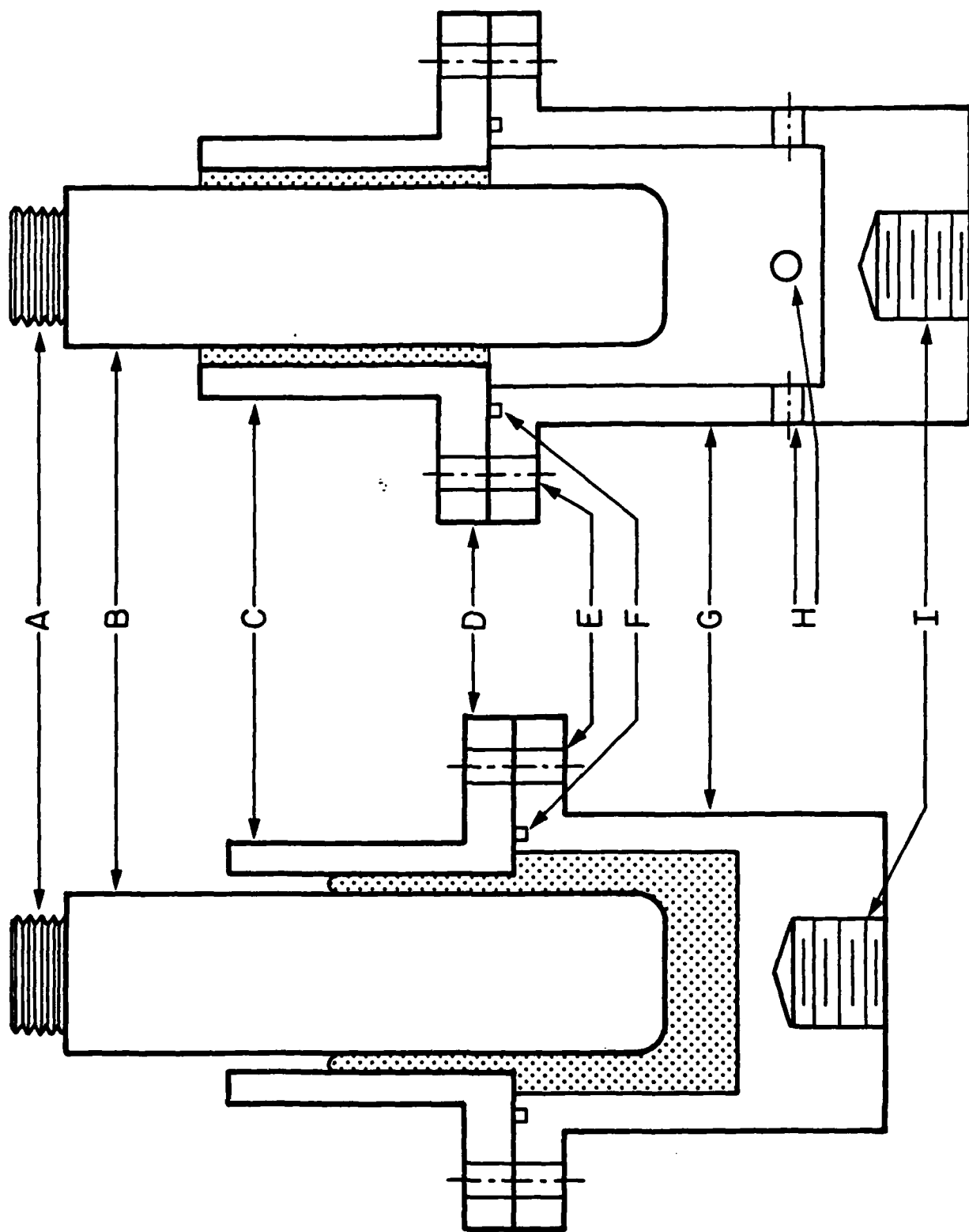16. D.S. Soong and M. Shen, J. Rheology $\underline{25}$, 259 (1981).

17. T.Y. Liu, D. S. Soong and M. C. Williams, J. Rheol. $\underline{27}$, 7 (1983).

18. T.Y. Liu, D.S. Soong, and M.C. Williams, Polymer Preprints, $\underline{23:2}$, 42 (1982).

19. N. Sivashinsky, A.T. Tsai, T.J. Moon and D.S. Soong, submitted to J. Rheol.

20. A.W. Myers and J.A. Faucher, Trans. Soc. Rheol., $\underline{12}$, 183 (1968).

21. R.V. McCarthy, J. Rheol., $\underline{22}$, 623 (1978).

22. T. L. Smith, J.D. Ferry and F.W. Schremp, J. Appl. Phys., $\underline{20}$, 144 (1949).

23. E. Ashare, R.B. Bird, and J.A. Lescarboura, A.I.Ch.E. J. $\underline{11}$, 910 (1965).

24. R.J. McLachlan, J. Phys. E., $\underline{9}$, 391 (1976).

25. F. Ramsteiner, Rheol. Acta, $\underline{15}$, 427 (1976).

26. K.K. Chee and A. Rudin, Can. J. Chem. Eng., $\underline{48}$, 362 (1970).

27. K.K. Chee and A. Rudin, Rheol. Acta $\underline{16}$, 635 (1977).

28. A. Rudin, C.K. Ober, and K.K. Chee, Rheol. Acta, $\underline{17}$, 312 (1978).

Figure Captions

Fig. 1   Block diagram showing the various components of the SCR/MTS
         system. The strain program generated by the function generator is
         translated into actuator movement via constant monitoring of the
         LVDT signal by the servocontroller. The force produced by the
         fluid is measured with the load cell. Both stress and strain
         signals are continuously recorded by any one of the three output
         devices.

Fig. 2   Detailed (although not drawn to scale) diagrams of the sliding
         cylinder rheometer. A full cup is used for sample loading (left),
         whereas a perforated one with large holes is used for actual
         testing to eliminate air resistance (right). A: threaded neck for
         attachment to the load cell; B: inner rod; C: outer cylinder; D:
         flanges; E: bolts for fastening flanges; F: O-ring; G: cup; H:
         holes to eliminate air dynamics; I: threaded neck for attachment
         to the actuator.

Fig. 3   Steady-state viscosity as a function of shear rate for the 20% by
         wt. PIB-in-decalin solution. Circles are data by SCR, whereas
         triangles are data by PPR (13). Results from both devices were
         accumulated over several runs on different days.

Fig. 4   Comparison of the results of stress growth and relaxation
         experiments performed on the 20% PIB solution using PPR and SCR.
         The top curve gives the shear strain history of this transient
         test. The PPR stress trace shows small fluctuations when the
         plates undergo relative motion, whereas the SCR stress trace is
         reasonably free of noise. This smoothness of output signal is
         possible because the SCR design does not entail any moving parts
         in contact.

Fig. 5   Strain and stress traces for a shear-rate-reduction experiment. A
         distinct stress undershoot is observed immediately following shear
         rate reduction.

Fig. 6   Strain and stress traces for a shear-rate-increase experiment.
            Two stress overshoots are seen accompanying the step changes in
            shear rate.

Fig. 7   Strain and stress histories of an interrupted flow. During the
            rest period, stress relaxes to vanishing values, yet the second
            stress overshoot peak is noticeably lower than the first one.

Fig. 8   Stress vs. strain curve for a large-amplitude oscillatory
            experiment with strain amplitude of 3 strain units. The dotted
            curve represents the first cycle when the fluid is first set in
            motion after a long rest period, while the solid curve gives the
            steady state behavior. These Lissajous curves spiral inwards from
            the start of the experiment to approach the steady state
            asymptotically, signifying progressive alternation of fluid
            structure.

Fig. 9   Stress vs. shear rate curve for the large-amplitude oscillatory
            flow depicted in Fig. 8. Only steady-state cycle is shown here.
            Fluid nonlinearity results in a nonelliptical curve.

Fig. 10   A crude sketch outlining the different flow regimes encountered in
            a falling cylinder device. The exact radial velocity profile in
            the annular spacing is dictated by the rheological properties of
            the test fluid. Converging and squeezing flows near the bottom
            also contribute to the force required to achieve rod movement.

Testing

Loading

A
B
C
D
E
F
G
H
I

20.0 wt% PIB-decalin

o SCR
▲ PPR

Log $\dot{\gamma}$ (sec^{-1})

Log η (Pa·s)

Pressure
and
Drag Flow

Converging
Flow

Squeezing Flow